Journal of Mining and Environment (JME) Vol. 16, No. 2, 2025, 633-651

Shahrood University of Technology

Journal of Mining and Environment (JME)

Journal homepage: www.jme.shahroodut.ac.ir

Iranian Society of Mining Engineering (IRSME)

The utilization of Convolutional Neural Network for the analysis of Spectral Induced Polarization data through inversion techniques

Parnian Javadi sharif[1], Ali Reza Arab-Amiri [2]*, Behzad Tokhmechi[3], and Fereydoun Sharifi[4]

1. Faculty of Mining, Petroleum & Geophysics Eng., Shahrood University of Technology, Shahrood, Iran
2. Post Doctoral Researcher, University of Cologne, Cologne, Germany

Article Info

Received 16 May 2024
Received in Revised form 29 August 2024
Accepted 31 August 2024
Published online 2 October 2024

DOI: 10.22044/jme.2024.14527.2734

Keywords

SIP
CNN
GEMTip
CLR
LOGratio

Abstract

The technique referred to as Complex Resistivity (CR) or Spectral Induced Polarization (SIP) possesses the capability to distinguish between various kinds of minerals or the sources of induced polarization by utilizing the physical characteristics of minerals or polarizable inclusions. The Generalized Effective Medium Theory of Induced Polarization (GEMTip) model is utilized to derive physical characteristics from SIP data. Different inversion methods are applied for this task, though they encounter difficulties such as computational costs, non-linearity, and the intricacy of the inverse issue. To tackle this, a new inversion approach based on Deep Learning (DL) via Convolutional Neural Network (CNN) is proposed for predicting the parameters of polarizable particles from SIP data. The CNN is trained on 20000 synthetic datasets produced using the GEMTip forward model. While DL networks address non-linearities, specific modifications are applied to synthetic datasets to evaluate the influence of non-linearity and correlation on the results. In the Kervian region southwest of Saqqez city, gold mineralization is linked to quartz and pyrite minerals, with two types of pyrite recognized - coarse-grained barren and fine-grained auriferous. The existence of sulfide mineral pyrite, along with variations in pyrite sizes, presents an attractive target for SIP exploration in the investigated area. The trained network is also validated on Gravian data and effectively retrieves parameters as evidenced by the data. The proposed methodology simplifies the inversion process by estimating parameters in one step, enabling a direct and efficient procedure.

1. Introduction

The complex Resistivity (CR) or Spectral Induced Polarization (SIP) method is capable of distinguishing the type of minerals or the sources of induced polarization by using the physical characteristics of minerals or polarizable inclusions. Because of this ability, it has a wide application in the exploration of minerals and hydrocarbon resources [1,2,3,4,5,6,7] environmental studies [8, 9], hydrogeology [10].

To obtain physical characteristics from SIP data, different relaxation models are used; the most common relaxation models are Cole-Cole [1] and the Generalized Effective Medium Theory of induced polarization (GEMTip) [5]. Cole-Cole model considers the resistivity as the bulk system and does not notice the composition of the system [1], while the GEMTip model gives the relationship between rock composition and complex resistivity/conductivity based on the Effective Medium theory (EMT) [5]. To determine the petrophysical properties of the rock, the GEMTip relaxation model is used.

The GEMTIP model provides an integrated mathematical method to study the heterogeneity of multi-phase structures and the induced polarizability of rocks. The geoelectrical parameters of the combined conductivity model are determined using the inherent physical and geometric characteristics of the rock material composition, such as mineralization or rock fluid content, matrix composition, porosity, anisotropy, and polarizability of the compositions. GEMTIP

* Corresponding author: alirezaarabamiri@yahoo.com (A.R. Arab-Amiri)

model parameters are not only chargeability (m), frequency dependence (c), time constant (τ) and resistivity of matrix (ρ_0) but also volume fraction of grains (f), resistivity of grain (ρ_i), size of grain (a) and polarization coefficient (α) [5].

One of the basic problems of conventional relaxation models (Cole-Cole and GEMTIP), which makes the process of modeling and retrieving its parameters a serious problem, is the correlation between the parameters of the model [11]. Previous studies show a strong correlation between chargeability(m) and frequency dependence(c) in both real and synthetic data [12]. The relation between chargeability (m) and volume fraction of grains (f) is non-linear, while polarizability parameters and anisotropy affect chargeability (m) and time constant [13]. To reduce the effect of these correlations between parameters, [14] conduct reparameterization on Cole-Cole relaxation model parameters.

As Jackson and Matsu'Ura [15] and Ivanov [16] show, the existence of non-uniqueness cannot be eliminated from the geophysics inverse problem, so they concluded that the parameter space formed a closed (simplex) system in which adding or removing a parameter affects the other parameters. Therefore, using conventional statistical and mathematical methods and calculations to interpret data in Euclidean space may lead to misleading results [17,18,19]

Acquired SIP data reveal information about polarizable inclusions. This information is estimated by solving an inversion problem based on a chosen relaxation model where the SIP data are inputs and the model parameters are outputs. For this purpose, the inversion method is applied to the data and relaxation forward model. Inversion methods are divided into two main categories: 1) deterministic and 2) probabilistic methods. The deterministic method can estimate parameters quickly, but different initial models lead to the same results caused by non-uniqueness issues. Probabilistic methods considering the problem's non-linearity are computationally expensive [20]. Probabilistic inversion methods were simplified using Artificial Neural Network (ANN), then the forward model was replaced by trained data. Using machine learning (ML) reduces the algorithm's convergence time [21]. Deep Learning (DL) is a method of ML that is approved to be robust for data analysis [22,23]. DL inversion strategy based on Convolutional Neural Network (CNN) utilized for 1D electromagnetic data inversion [20,24].

The emergence of contemporary data acquisition and storage technologies has resulted in a substantial augmentation of data volumes, with both conventional and machine learning methodologies grappling to effectively process, manage, and analyze the extensive quantities of data now accessible. The mineral exploration sector is certainly not exempt from this big data dilemma. Decision-making in exploration has become significantly more intricate in the context of big data, particularly concerning inquiries about optimal strategies for managing and utilizing the data to derive information, cultivate knowledge, and achieve insight. One of the methodologies employed by the mineral exploration sector in addressing big data is the utilization of geographic information systems (GIS). For instance, GIS platforms are frequently employed for the integration, interrogation, and interpretation of various geoscience and mineral exploration datasets, with the objective of refining and prioritizing known targets and identifying new prospects [25]. As scientific inquiry necessitates both practicality and applicability to secure its efficacy; this involves the capability to distinctly articulate its fundamental nature. Accordingly, in research characterized by experimental methodologies, it is imperative to possess the competence to observe, quantify, and execute experiments. The trajectory of scientific exploration adheres to methodical procedures; thus, maintaining an organized framework and order during the various stages of the research is critical for its successful execution, as it fosters the effective allocation of temporal, financial, human, infrastructural, and instrumental resources. Furthermore, the essential elements of data acquisition, categorization, analysis, deduction, and achieving a precise comprehension of the dilemma are crucial for rendering scientific research feasible and attainable. Consequently, it is essential to choose any form of scientific inquiry in a manner that permits systematic implementation. Consequently, it is imperative to select a methodology for scientific inquiry that facilitates systematic execution; thus, the application of Exploration Information Systems (EIS) has gained considerable traction in recent years[26].

This paper's main purpose is the correlation between parameters and their effect on inversion results. Therefore, the asset of 20,000 synthetic data was generated using the GEMTIP relaxation model. Independent parameters are generated randomly, and dependent parameters are calculated based on independent parameters to implement correlations among parameters. Non-uniqueness issues are considered as a result of simplex space

of parameters. Logratio transformation is applied to transform parameters from Simplex space to Euclidean space. CNN has been trained in different prepared synthetic data (original form and log-ratio transformed).

Regarding the performance of the trained Network, the best-trained Network was chosen to apply synthetic and real data. This paper proposes applying a DL network via CNN to conduct an inversion of SIP data and extract features and parameters from data. Also, considering the correlation of parameters involved is the novelty of the paper.

2. Methods

2.1. Geology

This geological map is used as a basic tool for the purpose of gold exploration in the area. Since tectonics has been so active in the entire region enclosing the studied area, the initial stratigraphic relations have been disrupted by its performance. In general, the outcropped deposits in the area can be divided into the two main sedimentary and igneous parts, both of which have been transformed into the green schist facies (Figure 1).

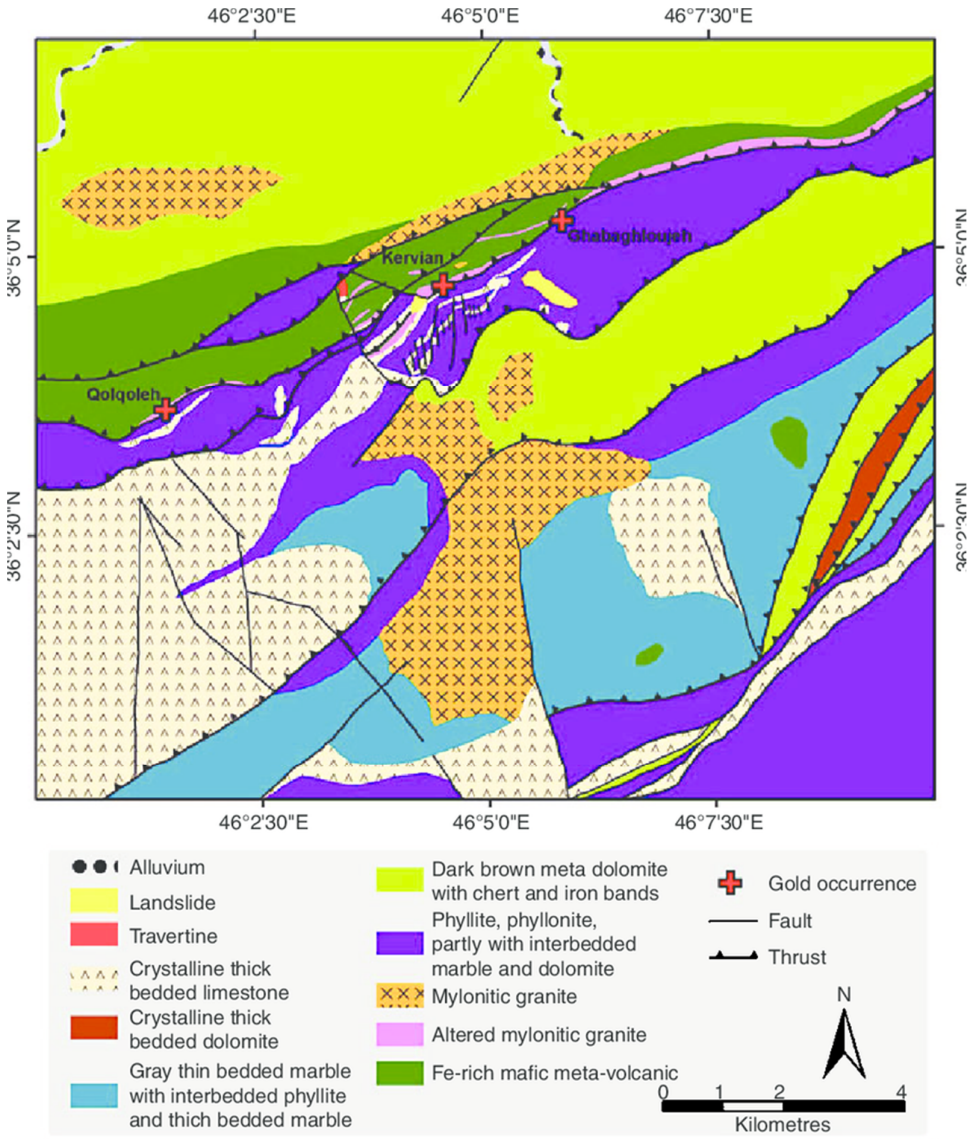

Figure 1 illustrates a geological map of the Kervian region. The geological map, created by Mohajjel [27], also highlights tectonic elements like faults.

Sedimentary deposits are characterized by the presence of carbonate minerals such as limestone, metamorphic dolomite, and peltic sediments that have undergone metamorphism to form phyllite.

This diverse array of sedimentary rocks provides valuable insights into the geological processes that have shaped the Earth's surface over millions of years. Additionally, the igneous rock assemblage found in this region is composed of both volcanic and intrusive rocks, exhibiting a unique blend of acidic and alkaline compositions, resulting in the formation of schists with distinctive mineralogical characteristics.

The division of faults in the region can be categorized into various types, with thrust faults being the most significant among them. These thrust faults are responsible for the repetition of lithological units, a crucial aspect of the region's geological makeup. Detecting these faults within volcanic mylonite units poses a considerable challenge due to their parallel nature and similar slope to the predominant mylonite foliages. Nonetheless, in areas where a sedimentary assemblage is present, the identification of repeated lithological units becomes feasible. Therefore, the presence of different lithological units in such regions can aid in the recognition of fault patterns and geological formations [28].

Gold mineralization in the Kervian area is evident in two distinct forms, namely vein/veinlet type and disseminated mineralization. The presence of mineralization within the siliceous units, which exhibit varying thickness ranging from 1-2 cm to several meters, is characterized by laminates and veins that run parallel to the orientation of mylonite units. Conversely, in the highly silicized wall stones, the mineralization is predominantly disseminated throughout the rock matrix. [29]

The examination of the association between the outcomes of assay evaluation of the specimens collected from the trenches situated in the metamorphic and mineralized regions with varying rock formations reveals a robust connection between the elevated levels of gold with extensively deformed units such as mylonite and ultra mylonite, alongside altered units like siliceous and sulfide-carbonate, and metamorphosed volcanic units of an acidic nature. Consequently, a remarkably proximate spatial correlation is discernible between the hydrothermal modification in conjunction with ductile shear deformation and the process of mineralization. Broadly speaking, mineralization tends to manifest within the faulted, deformed, modified, and metamorphosed geological units, where the geological dynamics have exerted a substantial influence and have impacted the mineralization phenomena within the locale [29].

In the recent years, several research initiatives have been carried out by the Gold Exploration Division within the Geological Survey of Iran with the aim of exploring gold deposits in the Kervian region, some of which have resulted in extensive exploration activities and supplementary investigations. Preliminary exploration endeavors conducted until 2001 in the Saqez locality unveiled the presence of gold anomalies in the Kervian and Gholgholeh regions. During the autumn of 2001, the excavation of seven trenches spanning a cumulative length of 500 meters, along with the retrieval of 138 samples from these sites, led to the identification of seven veins within the Kervian area [29].

In the research conducted, our case study was carried out specifically in the Kervian region situated in the southwestern part of Saqqez city, which lies to the northwest of the Sanandaj-Sirjan zone. The study zone under scrutiny reveals a notable connection between gold mineralization and quartz alongside pyrite minerals. This area showcases a distinctive presence of two types of pyrite minerals, namely the coarse-grained unproductive variety and the fine-grained auriferous mineral. The existence of sulfide mineralization, particularly in the form of pyrite mineral, as well as the stark contrast in the dimensions of pyrite minerals, serves as a prime focal point for Spectral Induced Polarization (SIP) investigation. The intricate interplay between the occurrences of various minerals and their characteristics within the study area offers a rich tapestry for further exploration and analysis. Investigating the properties and distributions of these minerals can provide valuable insights into the geological processes at play in the region. The utilization of advanced techniques such as SIP can enhance our understanding of the mineralization processes and aid in the identification of potential mineral deposits in the Kervian area. After obtaining samples from the specified mineral deposit, they were sliced into cylindrical segments measuring 2 cm in both diameter and length. Subsequently, following the standard laboratory procedures for preparation, the composite specific resistance was determined using the SIP Fuchs 3 instrument within the frequency spectrum spanning from 1.46 mHz to 20 kHz. The results of one of these measurements are detailed in the accompanying table 1, providing valuable insights into the electrical properties of the mineral samples analyzed.

Table 1 response of SIP Fuchs 3 instrument in some ferequencies between 1.46mHz to 20KHz

Sfreq(Hz)	$\rho(\omega)$	Phase(mr)	dR(%)	dP(mR)
20000	8/90E+04	7/46E+04	-566/983	0/01
3000	1/08E+05	9/04E+04	-112/859	0/0158
750	1/10E+05	9/21E+04	-36/5411	0/0147
187/5	1/11E+05	9/30E+04	-16/6159	0/0089
46/875	1/12E+05	9/38E+04	-11/387	0/0551
11/71875	1/13E+05	9/46E+04	-9/7861	0/0071
2/929687	1/14E+05	9/54E+04	-8/8035	0/0076
0/366211	1/15E+05	9/65E+04	-7/3087	0/0264
0/045776	1/17E+05	9/77E+04	-6/195	0/0981
0/001431	1/20E+05	1/00E+05	-6/3513	NaN

2.2. Spectral induced polarization

In the spectral induction polarization method, in a wide frequency range (0.001 to 104 Hz), the amplitude and phase (or real and imaginary components) of the complex resistivity are measured as a function of the frequency. The measurement of these two parameters provides the possibility of checking the frequency dependence by using a suitable relaxation model, and by using it, valuable physical information about rock and subsurface anomalies is obtained. In the presence of the induced polarization effect, the measured potential in the frequency domain is a complex parameter [8] . Therefore, the resistivity is a complex number in the form of Equation (1).

$$\rho(\omega) \quad = \rho_{real}\ (\omega) + i\rho_{imag}\ (\omega) \qquad (1)$$

Where The phase angle is calculated from the Equation (2).

$$\phi = \tan^{-1} v_{imag}/v_{real} = \tan^{-1}(\rho_{imag}/\rho_{real}\ ) \qquad (2)$$

In order to check the frequency dependence of electrical characteristics, it is necessary to express their spectral behavior quantitatively. Different methods exist for this purpose, such as the Cole-Cole and GEMTIP relaxation model.

The GEMTIP model for the effective resistivity ρ_e related to the multi-component composite material with spherical grains will be in the form of Equation (3)

$$\rho_e = \rho_0\ \{1 + \sum_{l=1}^{N}\left[f_l\ m_l\ \left[1 - \frac{1}{1 + (i\omega t_l)^{c_l}}\right]\right]\}^{-1} \qquad (3)$$

Where:

$$m_l = \frac{3\ (\rho_0 - \rho_1)}{(2\rho_1 + \rho_0\ )}, \tau = \left[\frac{a_l}{2\alpha_l}(2\rho_l + \rho_0\ )\right]^{\frac{1}{c_l}} \qquad (4)$$

In these equations, ρ_0 is the resistivity of the matrix, f_i is the volume percentage of each type of grain, m_i is the load capacity of the grains, a_i is the average size of the grains, α_i is the polarizability coefficient of each of the grains, τ_i is the time constant, and c_i is the frequency dependency of each grain [5].

2.3. Log ratio transformation

In many problems, the sampling space includes components, all or most simplex data.

$$S^d = \{(x_1, x_2, \dots, x_d): x_i > 0 (i = 1,2, \dots, d), \{\sum_{i=1}^{d} x_i < 1\} \qquad (5)$$

In these problems, the concept of independence plays an important role in statistical analysis. Since the simplex is weak in the independent of components, correlation measurement, and the absence of distribution class parameters in the S*d* space, they are unsuitable for statistical analysis. Aitchison presented concepts of independence in the simplex space to establish a connection between the existing concepts and to develop new and strong parametric classes of the distribution of statistical analysis methods [17].

The transformation of the central root logarithm for the D-dimensional of x composite sample is done in Equation (6) by [17].

$$y = (y_1, y_2, \dots, y_D) = \left(\log\left(\frac{x_1}{\sqrt[D]{\left(\prod_{i=1}^{D} x_i\right)}} \right), \log\left(\frac{x_2}{\sqrt[D]{\left(\prod_{i=1}^{D} x_i\right)}} \right), \dots, \log\left(\frac{x_D}{\sqrt[D]{\left(\prod_{i=1}^{D} x_i\right)}} \right) \right) \quad (6)$$

Where y_i is the variable value in the regular system, calculated using central root logarithm transformation.

CoDaPack (a R package to study and work with compositional data) is employed in this study to conduct log-ratio transformations.

2.4. Convolution Neural Network (CNN)

The function of neural networks is to imitate the human brain, and the convolutional neural Network (CNN) is no exception to this rule. These neural networks analyze and extract details, regression, and classification by simulating neurons and processing layers. CNN consists of three important layers: 1) the convolutions layer, 2) the pooling layer, and 3) the fully connected layer [22,23,30].

Convolution layer: This layer extracts input features using filters. This layer consists of the concept of filter, step, and layer. The function of filters is to form a feature table with point multiplication and a selective filter in the data. Filters are also called kernel or feature detection. In this layer, different filters are used according to the need of the filter, and after applying filters, it uses an activator function. The RELU (rectified linear unit) function is the most used activator function. Steps: Specifies the number of filter steps, which reduces the size of the output table. The higher the number of steps, the smaller the feature table size and the lower the accuracy. However, more steps should be considered regarding reducing the calculations. Layering: is called to be accurate in data mining and remove the border effect according to the subject type; this process adds a zero value (zero padding) and increases attention to the main data.

Pooling layer: In this layer, the filter is applied to the attribute table, and the steps are selected so there is no overlap. This layer reduces the boundaries and increases the speed of reducing the volume of calculations and a summary of features considered. The method of this layer is based on maximum data or average aggregation [30] .

Fully connected layers: The flattening process is done to connect the output to fully connected layers. After this step, one or two layers will be completely connected in the next step. Finally, the convolutional output is defined and classified depending on the type of Network. It is strengthened and connected to the fully connected layers to produce the output value according to the active function, and thus, the Network is trained [20,30].

2.4.1. Convolutional neural network architecture

The number of parameters in CNN is large, so one of the most important issues is designing a suitable architecture. In architectural design, the impact on accuracy and speed is one of the most effective and widely used factors in the last 10 years. In architecture, several separate layers are usually used. The most famous architectures used are Lenet, Alexnet, VGG, Googlenet, inception v3, and ResNet-50. In this research, a one-dimensional CNN algorithm is considered on inputs and outputs; the inputs are the data values of the complex resistivity at different frequencies, and the outputs are the model parameters Figure 2.

resistivity and SIP parameters, respectively (based on trained model using net2vis tool)

This structure conducted using [20] includes two sets of convolutional layers; the first layer includes four convolutional layers with a filter size of (kernel size) 2 and stride of 1, and each convolutional layer is followed by pooling layers and the leaky-ReLU activation function with the leakage coefficient of 0.01 was used in each convolution. The first part of the algorithm takes the input with dimensions 1*25 (complex data) and gives the output matrix 2*675 (the number of filters started from 25 in the first layer and then enhanced by a factor of 2 after each max pooling layer).

The second convolution layer consists of 3 layers with 24, 12, and 6 filters, respectively. Like the previous layer, activation is done using the leaky-ReLU function. This set of layers reduces the size of the detail map and presents the result matrix as a vector of parameters in relation to the output layer. The remarkable point about this network is the possibility of replacing the second set of layers. In classical fully connected layers, each neuron is connected to the previous layer with weights, and feature extraction does not work well.

In contrast, in convolution layers, each neuron is connected to only a few neurons of the previous layer, and the convolutional operator allows extracting details from data. Considering this feature, convolutional layers are more effective than fully connected layers. The second set of convolution operators is more effective at this stage than fully connected networks by reducing the data set Moghadas [20]

Dürr [37] introduces three Deep Learning Uncertainty Quantification (DL-UQ) techniques, specifically referred to as FPCNN, DEPCNN, and BPCNN. These methods are meticulously crafted to assess both aleatoric and epistemic uncertainties within neural networks. Each of these three approaches leverages intricate mechanisms such as weight perturbation matrices, training with multiple model weights, and implementing probability distributions for both weights and biases. The primary objectives of these methodologies include the introduction of randomness to model weights through the use of weight perturbations and the accurate quantification of cognitive uncertainties by leveraging probabilistic distributions. Moreover, all three DL-UQ methods incorporate a probabilistic layer within the neural network architecture to produce outcomes following a normal distribution, facilitating the comprehensive evaluation of aleatoric uncertainty in the models. The application of the Keras function combined with the Tensorflow library plays a crucial role in minimizing uncertainty within the given process, ultimately leading to more precise and reliable outcomes for the tasks at hand. By leveraging the capabilities of these advanced tools, the complexity of the uncertainties involved in the process is significantly reduced, allowing for a more efficient and effective approach to problem-solving in various domains.

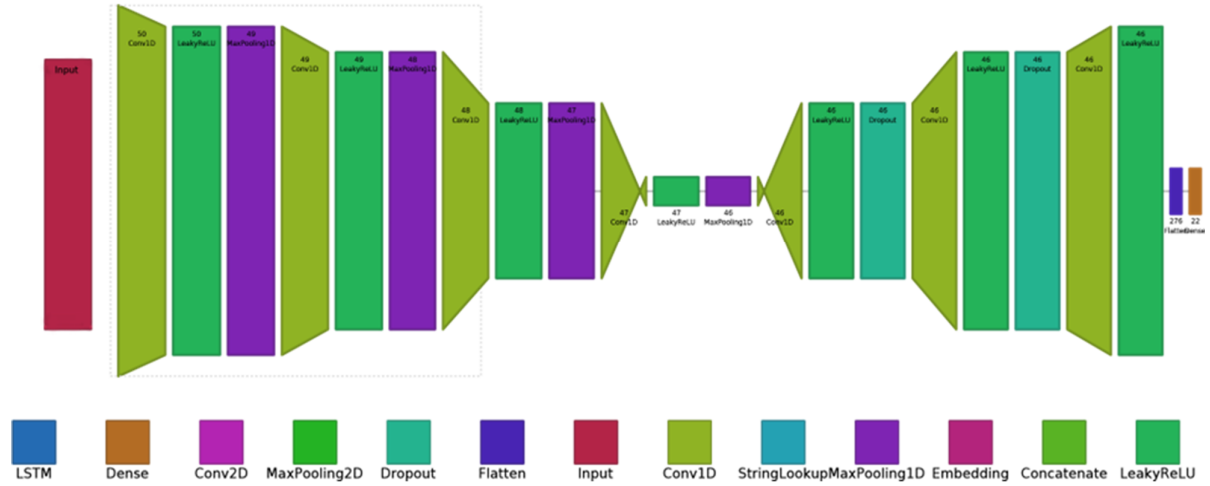

Figure 2. A fully convolutional neural network architecture. the input and output parameters are complex

2.5. Calculations and Results

Regarding simplex data and correlation of parameters and data, log ratio methods and linear and non-linear principal component analyses were used to reduce the dimension of parameters and compare the effect of each method on data analysis. Next, for inverting data, CNN applied as Moghadas [20] used for geophysics inversion problems and trained networks applied to experimental data.

The methodology utilized in this study integrates elements of randomness, dependency management, and machine learning methodologies to curate diverse ensembles. The commencement of the process involves the random generation of crucial parameters, setting the foundation for subsequent analyses. It is imperative to acknowledge that certain parameters exhibit interdependencies, wherein alterations in one parameter can significantly impact others within the system. To further enhance the robustness of the analysis, the parameters undergo scrutiny through the application of the GetMIP model, introducing a controlled level of noise at 5% to simulate real-world complexities. The subsequent phase involves the retrieval of parameters through the employment of a transformative approach, transitioning parameters from a simplex space to a Euclidean space, utilizing the CLR method. As the process unfolds, a Convolutional Neural Network (CNN) is deployed for training purposes, with the primary objective of reconstructing the outfit parameters with a heightened level of accuracy and precision. The iterative nature of these steps encapsulates a comprehensive approach towards

outfit generation, underscoring the importance of methodological diversity in computational fashion design. Through the amalgamation of diverse techniques and algorithms, this approach fosters a nuanced understanding of outfit creation, catering to the dynamic needs of modern fashion paradigms. The intricate interplay between randomness, dependencies, and machine learning mechanisms underscores the complexity inherent in outfit curation, necessitating a multifaceted approach towards computational fashion design.

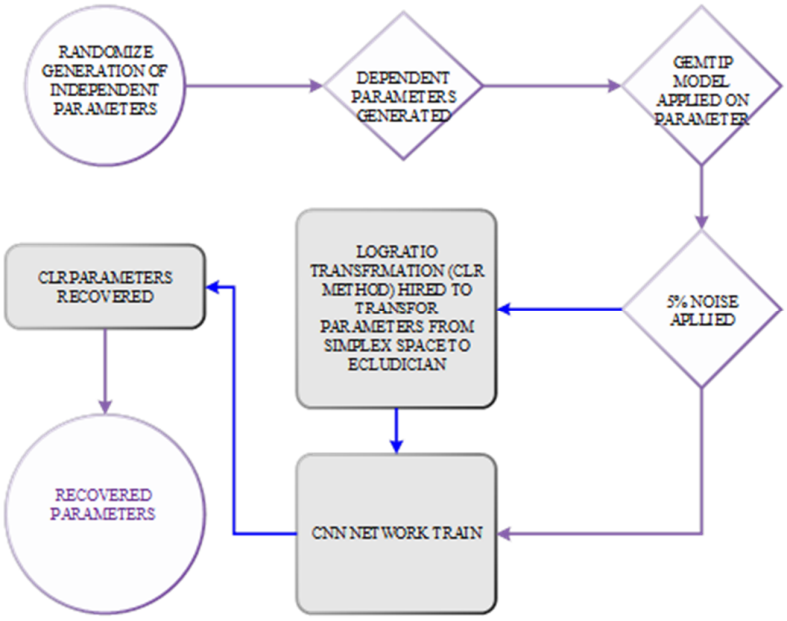

Figure 3 simple schematic of how methods combine for inversion solving

2.6. Synthetic data

Synthetic data was generated using known relation between dependent and independent parameters. To imply such a correlation in parameters, independent parameters (consist ρ_0, the volume fraction of polarizable particle, size of the particle, conductivity, and frequency-dependent coefficient of the particle) generated randomly and other parameters calculated based on mathematical models that describe the dependent parameters (Equations (4) and (7)):

$$e = \frac{a_x}{a_y}\ ,\ \overline{a} = \frac{a_x + a_y + a_z}{3} = \frac{(2 * e + 1)a_y}{3},\ \rho = \frac{1}{\sigma} \tag{7}$$

Hansen [21] suggested that Neural Networks require at least 5,000 training data; here, 20,000 training data have been used.

In this data set, the response values of the model at 25 frequencies are considered network input. 70% of the data was used to train the Network, and the remaining 30% was used to test and validate the Network. This data division is technically used for training and checking network performance.

3. Data Preparation

3.1. Correlation of parameters

In order to check the effect of each of the parameters on other parameters, the correlation table of the parameters (Table 2, 3) is presented. The right panel shows the correlation among parameters before any preparation, and the left panel is a correlation matrix describing the CLR transformation result. Regarding the correlation matrix Figure 4 and plot of parameters Figure 5, while CLR transformation decreases non-linearity through parameters, the linear effect of parameters increases where it is a much easier form of correlation form.

Also, as claimed, conventional statistic methods are unsuitable for simplex data space. Therefore, CLR transformation and change in the space of parameters cause the relationship between parameters to appear.

Table 2. correlation matrix between original parameters

	e	a	Rhoi	Rho0	tau	a1pha	c	m	f
e	1	-0.6	0.22	0.002	-0.09	-0.03	0.007	-0.03	0.007
a	-0.6	1	-0.18	0.009	0.27	0.07	-0.01	0.025	-0.005
rhoi	0.22	-0.18	1	-0.001	-0.12	-0.04	0.01	-0.098	-0.51
Rho0	0.002	0.009	-0.001	1	0.62	0.13	0.006	0.052	0.0001
tau	-0.09	0.27	-0.12	0.62	1	-0.47	0.61	0.038	-0.005
alpha	-0.03	0.07	-0.04	0.13	-0.47	1	-0.98	0.006	0.0095
c	0.007	-0.01	0.01	0.006	0.61	-0.98	1	0.002	-0.009
m	-0.03	0.025	-0.098	0.052	0.038	0.006	0.002	1	0.043
f	0.007	-0.005	-0.51	0.0001	-0.005	0.0095	-0.009	0.043	1

Table 3 correlation matrix between CLR transformed parameters

	e	a	Rhoi	Rho0	tau	a1pha	c	m	f
e	1	-0.7	0.3	-0.37	-0.26	-0.23	0.02	-0.14	-0.045
a	-0.7	1	-0.23	-0.09	0.23	-0.079	0.19	0.52	0.16
rhoi	0.3	-0.23	1	-0.17	-0.21	-0.14	0.02	-0.05	-0.51
Rho0	-0.37	-0.09	-0.17	1	0.57	-0.1	-0.043	-0.4	-0.13
tau	-0.26	0.23	-.21	0.57	1	-0.67	0.68	-0.11	-0.04
alpha	-0.23	-0.079	-0.14	-0.1	-0.67	1	-0.9	-0.42	-0.12
c	0.02	0.19	0.02	-0.043	0.68	-0.9	1	0.44	0.135
m	-0.14	0.52	-0.05	-0.4	-0.11	-0.42	0.44	1	0.31
f	-0.045	0.16	-0.51	-0.13	-0.04	-0.12	0.135	0.31	1

3.2. Log-ratio transformation

From the non-uniqueness problem of geophysics inversion, Jackson and Matsu'Ura [15] concluded that the parameter values of each of these models form a closed system, which means that these Values are relative and adding or removing a parameter from the set of model parameters affects the effect of parameters. Therefore, the use of conventional statistical and mathematical methods and calculations to interpret relevant data in the Euclidean geometric space leads to the production of wrong and misleading results [17,18,19]. To solve this problem, the data should be checked in Atchison's geometric space [17] using the operators and functions developed in this space or root logarithm transformations, including incremental logarithm transformation (ilr), central root logarithm transformation (CLR), and isometric root logarithm transformation (ilr)transformed the parameter values from the simplex and made it possible to work with them in the Euclidean geometric space [33]. Root logarithm transformations will be used to achieve this goal due to the conventionality of the second solution. In order to prepare the parameters for performing root logarithm transformations, considering that the closed values contain relative information, the sum of which becomes a fixed number (for example, 1, 100, 106), a feature related to the parameters should be defined, identified and extracted to meet these conditions. In other words, the sum of these features should equal a certain fixed value such as 1, 10, 100, or... For this purpose, a closer transforming function of the coda Package is applied to parameters that calculate the values based on Equation (8)

$$P_i = \frac{p_i}{\sum_{i \in N} P_i} * 100 \quad (8)$$

Where p_i is model parameters, N is the total number of parameters, and P_i is the percent of each parameter value.

Then, the CLR transformation was done on prepared data using CoDapack software. CoDapack has been developed for the statistical analysis of Compositional Data following the approach introduced by John Aitchison [34,35].

Figure 3 shows the effect of CLR transformations on parameters. The top panels show the parameters plot and the bottom panels are CLR transformations of parameters. Using CLR transformation causes a reduction of the parameter's range, which better clarifies the interaction between parameters. Plots Show dependency applied on parameters (Equations (4) and (7)) cause non-linear correlation while using CLR transformation omits non-linearity as seen in the plot. The time constant parameters are more complicated as more parameters are considered.

3.3. PCA extraction

The principal components have been extracted from the parameters using PCA and NLPCA methods [36] . In order to reduce parameters dimension, 3 principal components have been extracted and used to train the Network. Figure 4 shows the relationship between PCs in two linear and non-linear modes. The extracted PC values are used for network training.

The table 4 shows how extracted PCs and NLPCs cover the variance of parameters. R2 describes how PCs cover the variance. Based on the data PCs chosen, the higher value is more sophisticated. Cumulative R2 is used to choose the number of PCs; 3 PCs are considered to describe the data set.

PCA methods (NLPCA or PCA) reduce the correlation between parameters and introduce principal components. Figure 5 shows that linear methods are good for transforming data to CLR form, and the non-linear method worked well with the original parameters.

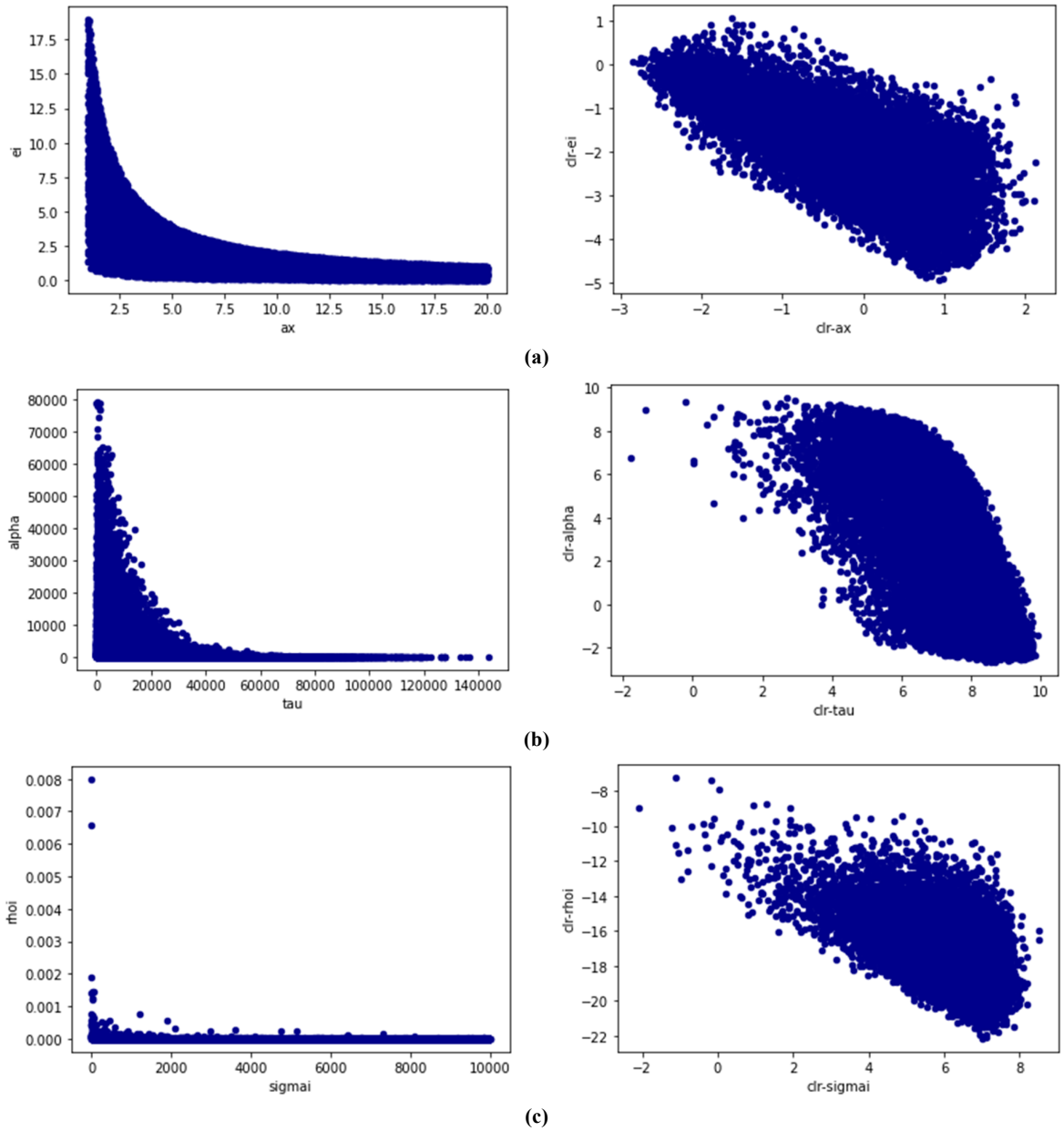

Figure 4. visualizing some correlation among parameters and CLR transformed A. size and shape correlation, B. polarization parameters of particle (α- τ) C. resistivity vs conductivity of particle.

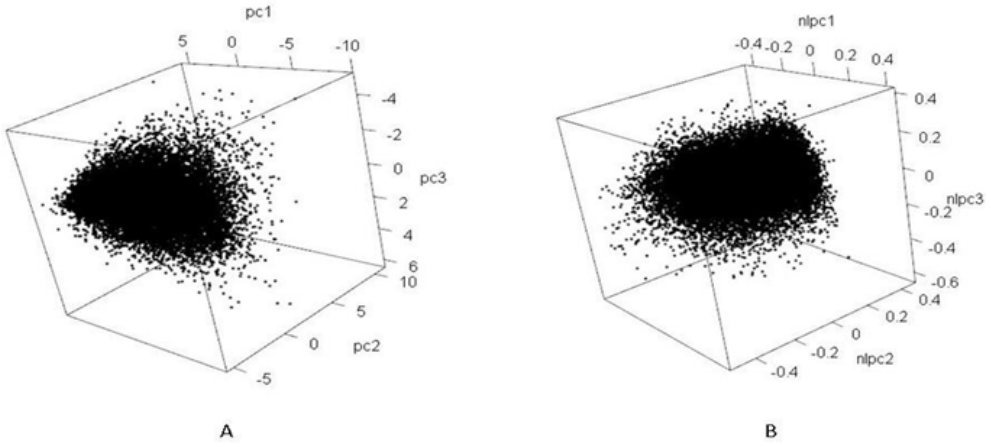

Figure 5. The relationship between the PCs. Panel A is the linear PCA method result, and panel B is the NLPCA method result. Both methods applied on CLR transformed form of parameters.

Table 4. PCs and NLPCs values of R2 and cumulative R2 to show how PCs were selected.

		PC1	PC2	PC3	NLPC1	NLPC2	NLPC3
Data	R2	0.8759	0.09884	0.016	0.9489	5e-6	0.00034
	R2 Cum	0.8759	0.9747	0.9907	0.9489	0.9489	0.94858
CLO	R2	0.6796	0.2506	0.051	0.8172	0.1071	0.00008
	R2 Cum	0.6796	0.9301	0.981	0.8172	0.9242	0.9234
CLR	R2	05479	0.2372	0.087	0.549	0.223	0.00065
	R2 Cum	0.5479	0.7851	0.782	0.549	0.7721	0.772

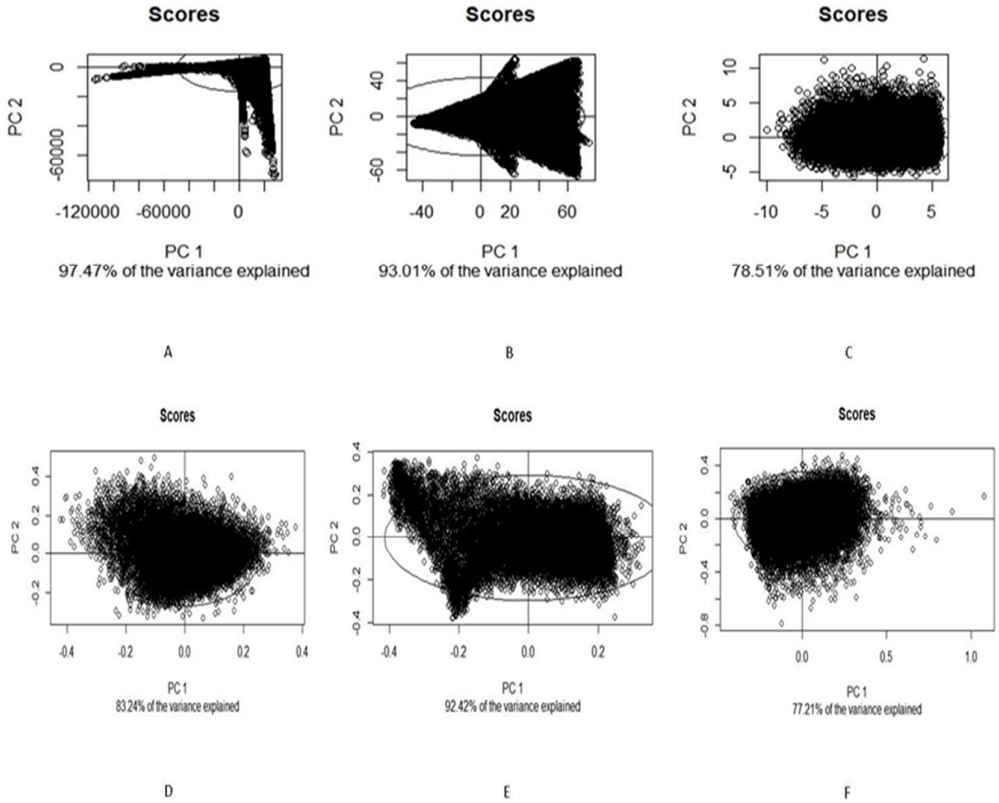

Figure 6. Scatter plot of PC scores to analyze how different methods reduce correlation. A, B, and C are PCs extracted using linear PCA. D, E, and F are PCs extracted by the NLPCA method. A and D were conducted on original parameters. B and E were conducted on CLO data (percent of each parameter among all parameters). C and F were conducted on CLR-transformed parameters.

Table 5. Loading matrix of parameters and PCs (method: linear PCA, inputs are CLR transformed parameters)

variable	PC1	PC2	PC
CLR-ei	0.050114093	0.269980726	0.356487875
CLR-ax	0.021213396	0.021213396	-0.094294971
CLR-rhoi	0.063595123	0.846835868	0.081248075
CLR-rho0	0.027534706	-0.069282311	-0.366341987
CLR-sigmai	0.032807769	-0.247427234	0.424455666
CLR-tau	0.278088267	-0.197006018	0.616532109
CLR-alpha	-0.908931699	-0.02376934	0.132430231
CLR-ci	0.292405661	-0.052042127	0.014481308
CLR-mi	0.034988643	-0.021322828	0.107778027
CLR-fi	0.03073315	-0.222068712	0.365484776

3.4. Network training

To train the Networks, synthetic data generated randomly were utilized. Training phase data (containing input and outputs) was standardized between 0-1 to avoid bias to specific variables. A total number of 5000 epochs was considered for the preparation utilizing the Adam algorithm [31]. The Adam algorithm ended up being computationally effective with a generally quick assembly rate [30].

The cost function has been reduced by using the least squares optimization algorithm. In total, 5000 iterations have been considered to optimize the optimization function, and the measurement units have been considered to check the CNN network with the names MAE (mean absolute error) and RMSE (root mean squared error). This measurement

compares model values (y^{mod}) with observed values(y^{obs}) with v data points.

$$MAE = \frac{1}{v}\sum_{i=1}^{v}\left|y_i^{obs} - y_i^{mod}\right|, RMSE = \sqrt{\frac{1}{v}\sum_{i=1}^{v}\left(y_i^{obs} - y_i^{mod}\right)^2} \quad (9)$$

3.5. Performance of the CNN

Calculating a variable as a cost function during the training phase helps to evaluate and check the network. The learning rate determines how fast the CNN is adjusted to solve the problem. In this regard, the non-stable and fast training rate indicates the inefficiency of the network. The graphs show the cost function versus the number of iterations in the training phase. The red and blue lines represent the value of validation and training, respectively.

Graph 1 shows network performance during the training procedure using RMSE and MAE and the histogram of training and validation errors. The blue and red lines present training and validation errors (top panel). Panels A, B, and C are the performance of the network trained by original parameters, closer form, and CLR transformation data, respectively. Panels D, E, and F are the performance of the network using linear PC extracted from original parameters, closer form, and CLR transformation data, respectively, and panels G, H, and I show the performance of the training network using non-linear PC extracted from original parameters, closer form and CLR transformation data respectively.

Graph 1 shows that while the algorithm planned to train in 5000 epochs, it works for almost less than 350 epochs. The graph shows that the best training procedure occurred when NLPCA was extracted from CLO (Graph 1 H), and original synthetic data (Graph 1 A) was used for training the CNN network. The network was selected based on time last for training procedure and error histogram. On the other hand, the training procedure works well for other data types.

3.6. Experimental Data

In the initial phase, the specimens under investigation underwent a thorough analysis focusing on their mineral composition and the process of identifying minerals capable of polarization. The range of minerals present comprises quartz, albite, orthoclase, muscovite, hematite, pyrite, rutile, calcite, ankerite, apatite, and monazite, with pyrite being the primary mineral with polarizable properties as highlighted by [31], while the remaining polarizable minerals are found abundantly. Despite their presence, these minerals are present in minimal quantities, thereby having negligible impact on the outcomes of

Spectral Induced Polarization (SIP) research investigations.

After obtaining samples from the specified mineral deposit, they were sliced into cylindrical segments measuring 2 cm in both diameter and length. Subsequently, following the standard laboratory procedures for preparation, the composite specific resistance was determined using the SIP Fuchs 3 instrument within the frequency spectrum spanning from 1.46 mHz to 20 kHz. The results of one of these measurements are detailed in the accompanying table 1, providing valuable insights into the electrical properties of the mineral samples analyzed.

Table 5 response of SIP Fuchs 3 instrument in some ferequencies between 1.46mHz to 20KHz

Sfreq(Hz)	$\rho(\omega)$	Phase(mr)	dR(%)	dP(mR)
20000	8/90E+04	7/46E+04	-566/983	0/01
3000	1/08E+05	9/04E+04	-112/859	0/0158
750	1/10E+05	9/21E+04	-36/5411	0/0147
187/5	1/11E+05	9/30E+04	-16/6159	0/0089
46/875	1/12E+05	9/38E+04	-11/387	0/0551
11/71875	1/13E+05	9/46E+04	-9/7861	0/0071
2/929687	1/14E+05	9/54E+04	-8/8035	0/0076
0/366211	1/15E+05	9/65E+04	-7/3087	0/0264
0/045776	1/17E+05	9/77E+04	-6/195	0/0981
0/001431	1/20E+05	1/00E+05	-6/3513	NaN

3.7. Inversion result

To check out the efficiency of trained model 2, the known model was used to gain and compare the model parameters with the real parameters. Table 6 shows the result of the inversion of models and expected values.

Table 6. inverted parameters and model parameters value

		rho0	m1	tau1	c1	f1	a1	m2	tau2	c2	f2	a2
Model1	Parameters1	6811	3	61633	0.97	22	16	3	23389	0.42	3.8	1.75
	CNNresult1	6879	3	64714	0.99	24	14.5	3	25026	0.44	3.7	4
Model2	Parameters2	1621	3	15375	0.85	20	14	3	86	0.003	33.4	18.6
	CNNresult2	1507	3	14606	0.87	21	12	3	87	0.0035	34	17.5

The best performance of trained CNN was selected and applied to SIP data reported by [33]. The sample contains two polarizable particles considered in training data. As [33] reported, the polarizable particle is pyrite with different polarizability characters.

Table 7 shows model parameters for 3 different samples in which polarizable extracted parameters describe the character of polarizable particles as expected.

Table 7. Inversion results using different data sets for training CNN

	rho0	m1	tau1	c1	f1	a1	m2	tau2	c2	f2	a2
Sample 1	5691	3	152	0.38	39	10.023	3	62	0.5	52	2
Sample 2	7901	3	183	0.59	58	13.03	3	70	0.65	30	2
Sample 3	5606	3	160	0.36	38	11.008	3	60	0.56	51	1

Graph 2 shows the response of forward modeling using estimated parameters (Table 5) and the experimental response of 3 real data sets in real, imaginary part, and ϕ. The last steep part of the data (right side) can be described as an effect of Electromagnetic coupling, which normally happens from a frequency of 500 Hz. So, measured data in larger frequencies are unreliable.

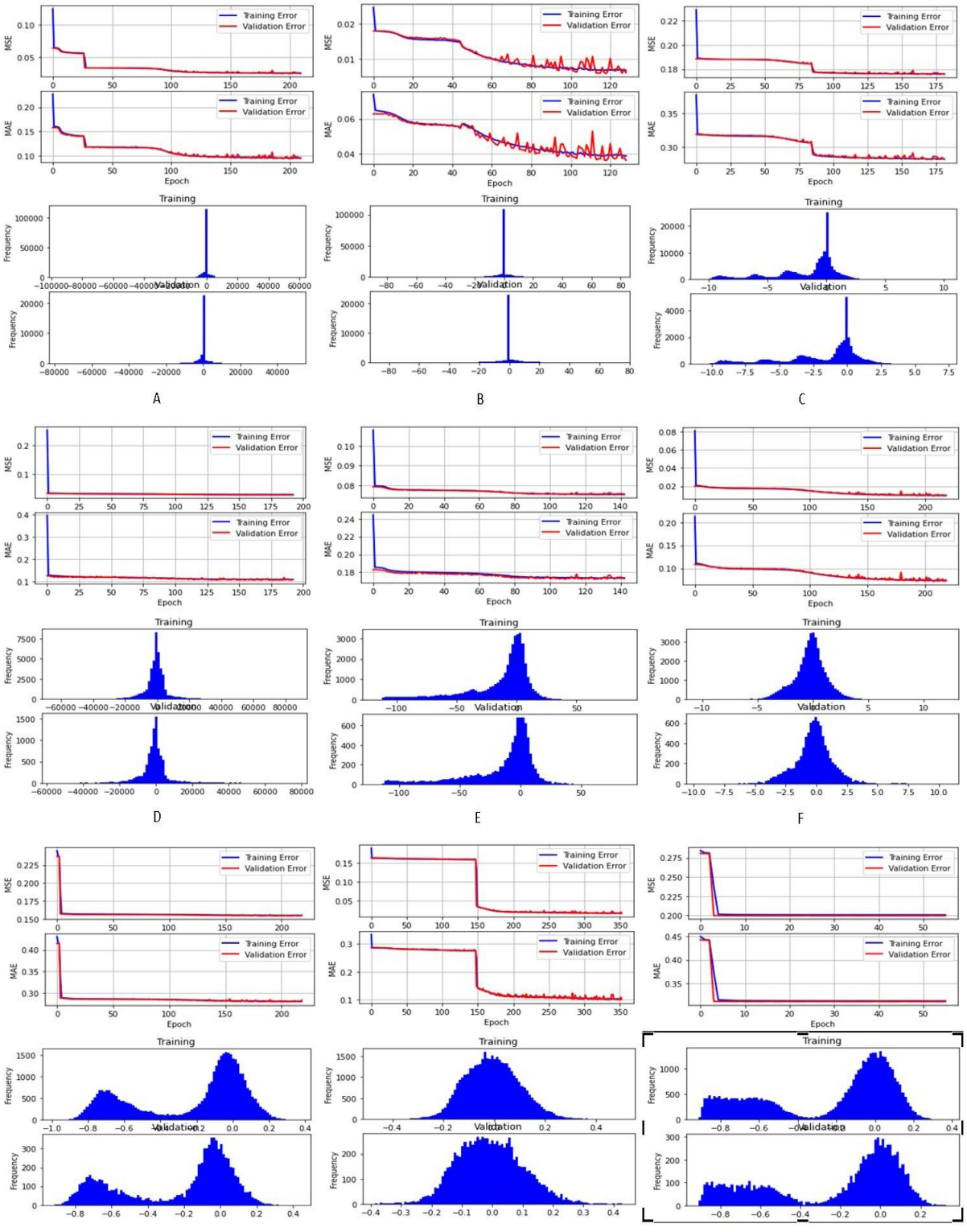

Graph 1. The performance of different data sets used to train networks. Two top graphs show RMSE and MAE, and the bottom graphs show the training and validation errors histogram, respectively. Panels A, B, and C are the performance of the Network trained by original parameters, closer form, and CLR transformation data, respectively. Panels D, E, and F are the performance of the Network using linear PC extracted from original parameters, closer form, and CLR transformation data, respectively, and panels G, H, and I show the performance of the training network using non-linear PC extracted from original parameters, closer form and CLR transformation data respectively.

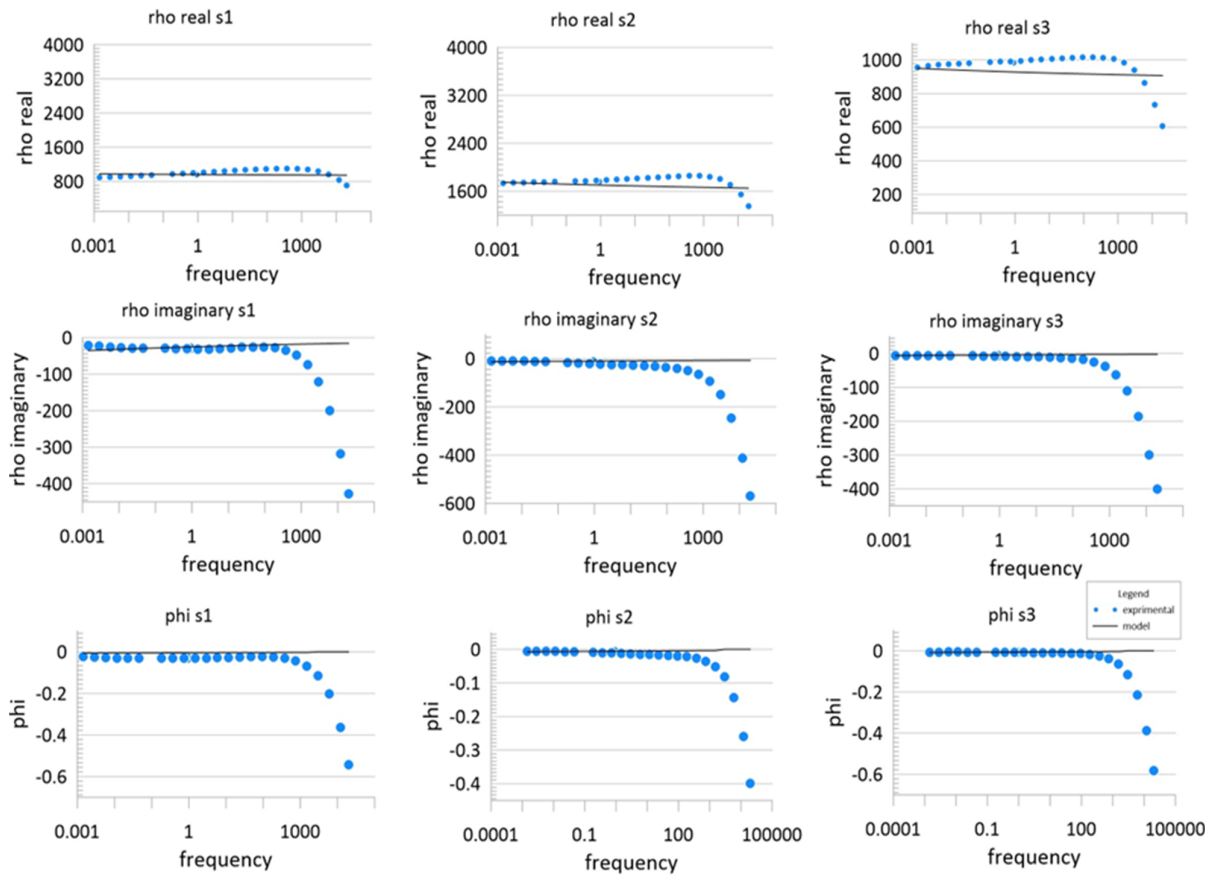

Graph 2. Comparing reproducing data using recovered parameters and experimental data for three samples.

4. Discussion

The utilization of the information combination tool presents a viable approach to handling uncertainty and enhancing decision accuracy. Effectively, merging information serves as a valuable technique for enabling the simultaneous integration of data from multiple sensors rather than relying on a single sensor. The benefits derived from employing multiple sensors encompass the duplication of information, reduction in measurement duration, enhancement of result reliability, and optimization of the signal-to-noise ratio. This approach facilitates a more profound reduction and control of uncertainty in decision-making processes, thereby furnishing a comprehensive overview of the environment and diminishing measurement expenses. Incorporating the proposed methodology as a pivotal component within the Exploration Information System, alongside findings from diverse techniques utilized in earth sciences like geological maps, satellite imagery, remote sensing data, geochemical survey data, and various geophysical methodologies, can significantly bolster the decisiveness of the decision-making process. This amalgamation of information sources contributes to a more robust decision-making framework, enabling a more informed and confident selection of actions. Ultimately, the synergistic integration of data from various sources through the information combination tool enhances the overall quality of decision-making processes, underscoring the importance of leveraging diverse sources of information in analytical frameworks. Thus, the strategic utilization of this tool within the realm of earth sciences can yield substantial improvements in decision-making outcomes.

Scientific research must be both feasible and applicable in order to ensure its success; this entails being able to clearly define its essence. Hence, in research of an experimental nature, it is crucial to have the ability to observe, measure, and conduct experiments. The process of scientific research follows systematic steps; thus, adhering to a structured approach and sequence in the various phases of the research is essential for its successful completion, as it enables the efficient utilization of time, finances, manpower, facilities, and tools. Moreover, the key aspects of data collection,

classification, analysis, inference, and gaining a precise understanding of the problem are vital for making scientific research practical and achievable. Therefore, it is imperative to select any type of scientific research in a manner that allows for orderly execution. The evolution of experimental techniques stemming from laboratory studies facilitates the application of these methods in industrial settings. In pursuit of this objective, laboratory SIP data underwent research and analysis to validate the proposed method. The samples prepared were subject to examination to assess their mineralogical characteristics and the composition under scrutiny within the simplex space being discussed. Subsequently, the investigation delved into understanding the influence of the simplex environment on data and parameters by identifying the samples and collecting SIP responses on a laboratory scale. To encompass all significant parameters in the SIP response, the Wahl's GEMTip model, which considers polarizability parameters and those linked to the physics of polarizable inclusions, was employed and scrutinized.

The use of CNN in inversion is synchronized with the correct training of the CNN, and this method can be used for both modeling and inversion of geophysical data and parameters. Here, to obtain the parameters related to the induced polarization factor, the Network is trained for inversion, and then to check the performance of the Network, the parameters are used to reproduce the model's response.

In general, network training is based on a limited number of polarization factors, and these simplifications aim to reduce the volume of DL network calculations. Since the Network is trained based on simplifications, this factor affects the inversion process, and recovered parameters follow the number of parameters used in training.

NLPCA and PCA methods have been used to reduce the number of investigated parameters. PC extracted with both linear and non-linear methods has reduced the volume of calculations, MSEA, and MRE. While NLPCA is more efficient, calculating non-linear PCs is time-consuming.

Using PCs for neural network training, it should be considered that synthetic data prepared for neural network training is made randomly, and the response of the GEMTip model to these values is considered; these simplifications affect the analysis.

Logarithmic transformations have been used to transform the data from the simplex space to Euclidean space, making it possible to use the data through conventional statistical methods.

In the DL method, using CNN, according to the network structure and the layers used, reduces the complexity of network inputs and outputs. It is also noteworthy that in the training stage of the Network, it is not necessary to use all possible models, but it is better to train with appropriate data in the appropriate range of model parameters.

5. Conclusions

In this article, a new method for inverting SIP data is proposed. This method implements a convolutional neural Network (CNN) on the data. In this implementation, logarithmic transformations and PC extraction have been performed on the input of the training network to check the effect of the simplex space and reduce the dimension of parameters.

This method saves time, reduces calculation volume, and provides inversion results in the shortest possible time. This capability is faster than probabilistic methods and even gradient-based methods and only requires many inputs. Also, the trained Network provides the desired parameter values without any initial intervention, which avoids the problem of nonuniqueness that occurs in other classical inversion methods. Also, this method can be widely used in geophysical studies and inversions. Using the transformed form of data (NLPCA, PCA, CLO, and CLR) causes more inversion stages to estimate the model parameters.

The complex interaction among the manifestations of different minerals and their attributes in the research site presents a diverse and intricate landscape that beckons for deeper investigation and scrutiny. Delving into the characteristics and spatial arrangements of these minerals has the potential to offer significant and valuable perspectives into the geological mechanisms at work within the vicinity. By employing sophisticated methodologies like Spectral Induced Polarization (SIP), we can enrich our comprehension of the mineralization procedures and facilitate the pinpointing of promising mineral reserves in the Kervian region. This amalgamation of mineral occurrences, their traits, and the application of cutting-edge technologies underscores the depth and breadth of opportunities for comprehensive analysis and exploration within the field of geology.

References

[1]. Pelton, W. H., Ward, S. H., Hallof, P. G., Sill, W. R., & Nelson, P. H. (1978). Mineral discrimination and removal of inductive coupling with multifrequency IP. *Geophysics*, *43*(3), 588-609.

[2]. Luo, Y., & Zhang, G. (1998). *Theory and application of spectral induced polarization*. Society of exploration geophysicists.

[3]. Emond, A. M. (2007). *Electromagnetic modeling of porphyry systems from the grain-scale to the deposit-scale using the generalized effective medium theory of induced polarization* (Doctoral dissertation, Department of Geology and Geophysics, University of Utah).

[4]. Goold, J. W., Cox, L. H., & Zhdanov, M. S. (2007). Spectral complex conductivity inversion of airborne electromagnetic data. In *SEG Technical Program Expanded Abstracts 2007* (pp. 487-491). Society of Exploration Geophysicists.

[5]. Zhdanov, M. (2008). Generalized effective-medium theory of induced polarization. *Geophysics*, *73*(5), F197-F211.

[6]. Sharifi, F., Arab-Amiri, A.R., Borner, R.U., Kamkar-Rouhani, A., (2018). Recovering IP effects from 1-D inversion of HEM data: case study from Kervian gold deposite (Iran), in: *AEM2018 7th international workshop on airborne electromagnetic.*

[7]. Sharifi, F., Arab-Amiri, A. R., Kamkar-Rouhani, A., & Börner, R. U. (2020). Development of a novel approach for recovering SIP effects from 1-D inversion of HEM data: Case study from the Alut area, northwest of Iran. *Journal of Applied Geophysics*, *174*, 103962.

[8]. Kemna, A. (2000). *Tomographic inversion of complex resistivity: Theory and application*. Der Andere Verlag.

[9]. Boerner, J. H., Herdegen, V., Repke, J. U., & Spitzer, K. (2017). Spectral induced polarization of the three-phase system CO2–brine–sand under reservoir conditions. *Geophysical Journal International*, *208*(1), 289-305.

[10]. Kemna, A., Binley, A., Cassiani, G., Niederleithinger, E., Revil, A., Slater, L., ... & Zimmermann, E. (2012). An overview of the spectral induced polarization method for near-surface applications. *Near Surface Geophysics*, *10*(6), 453-468.

[11]. Madsen, L. M., Fiandaca, G., Auken, E., & Christiansen, A. V. (2017). Time-domain induced polarization–an analysis of Cole–Cole parameter resolution and correlation using Markov Chain Monte Carlo inversion. *Geophysical Journal International*, *211*(3), 1341-1353.

[12]. Bérubé, C. L., Chouteau, M., Shamsipour, P., Enkin, R. J., & Olivo, G. R. (2017). Bayesian inference of spectral induced polarization parameters for laboratory complex resistivity measurements of rocks and soils. *Computers & Geosciences*, *105*, 51-64.

[13]. Gurin, G., Ilyin, Y., Nilov, S., Ivanov, D., Kozlov, E., & Titov, K. (2018). Induced polarization of rocks containing pyrite: Interpretation based on X-ray computed tomography. *Journal of Applied Geophysics*, *154*, 50-63.

[14]. Fiandaca, G., Madsen, L. M., & Maurya, P. K. (2018). Re-parameterisations of the Cole–Cole model for improved spectral inversion of induced polarization data. *Near Surface Geophysics*, *16*(4), 385-399.

[15]. Jackson, D. D., & Matsu'Ura, M. (1985). A Bayesian approach to nonlinear inversion. *Journal of Geophysical Research: Solid Earth*, *90*(B1), 581-591.

[16]. Ivanov, J., Miller, R. D., Xia, J., Steeples, D., & Park, C. B. (2005). The inverse problem of Refraction travel times, part I: Types of Geophysical Nonuniqueness through minimization. *Pure and Applied Geophysics*, *162*, 447-459.

[17]. Aitchison, J. (1982). The statistical analysis of compositional data. *Journal of the Royal Statistical Society: Series B (Methodological)*, *44*(2), 139-160.

[18]. Egozcue, J. J., Pawlowsky-Glahn, V., Mateu-Figueras, G., & Barcelo-Vidal, C. (2003). Isometric logratio transformations for compositional data analysis. *Mathematical geology*, *35*(3), 279-300.

[19]. Filzmoser, P., Hron, K., & Reimann, C. (2009). Principal component analysis for compositional data with outliers. *Environmetrics: The Official Journal of the International Environmetrics Society*, *20*(6), 621-632.

[20]. Moghadas, D. (2020). One-dimensional deep learning inversion of electromagnetic induction data using convolutional neural network. *Geophysical Journal International*, *222*(1), 247-259.

[21]. Hansen, T. M., & Cordua, K. S. (2017). Efficient Monte Carlo sampling of inverse problems using a neural network-based forward—Applied to GPR crosshole traveltime inversion. *Geophysical Journal International*, *211*(3), 1524-1533.

[22]. Shahriari, M., Pardo, D., Kargaran, S., & Teijeiro, T. (2022). Automated machine learning for borehole resistivity measurements. *arXiv preprint arXiv:2207.09849*.

[23]. Linting, M., Meulman, J. J., Groenen, P. J., & van der Koojj, A. J. (2007). Nonlinear principal components analysis: introduction and application. *Psychological methods*, *12*(3), 336.

[24]. Chen, X., Xia, J., Pang, J., Zhou, C., & Mi, B. (2022). Deep learning inversion of Rayleigh-wave dispersion curves with geological constraints for near-surface investigations. *Geophysical Journal International*, *231*(1), 1-14.

[25]. Yousefi, M., Kreuzer, O. P., Nykänen, V., & Hronsky, J. M. (2019). Exploration information systems–A proposal for the future use of GIS in mineral exploration targeting. *Ore Geology Reviews*, *111*, 103005.

[26]. Yousefi, M., & Hronsky, J. M. (2023). Translation of the function of hydrothermal mineralization-related focused fluid flux into a mappable exploration criterion for mineral exploration targeting. *Applied Geochemistry*, *149*, 105561.

[27]. Mohajjal, M., Eshragh, A., (2008). Geological map of Kervian area. *Geology survey of Iran*.

[28]. Ghazanfari, M, Fazli Khani, T. & Abbasi, Z. (2010). Report on public gold exploration in the area of Kervian. Geological Survey of Iran.

[29]. Najafi Ghoshebolagh, S., Kamkar Rouhani, A., Arab Amiri, A. R., & Bizhani, H. (2021). An Exploration Model for A Gold Deposit in Kervian Area, Kurdistan Province, Iran, using a Combination of Geophysical Results with Geological Information and Other Exploratory Data. *Journal of Mining and Environment*, *12*(2), 413-424.

[30]. Puzyrev, V. (2019). Deep learning electromagnetic inversion with convolutional neural networks. *Geophysical Journal International*, *218*(2), 817-832.

[31]. Kingma, D. P., & Ba, J. (2014). Adam: A method for stochastic optimization. *arXiv preprint arXiv:1412.6980*.

[32]. Telford, W. M., Geldart, L. P., & Sheriff, R. E. (1990). *Applied geophysics*. Cambridge university press.

[33]. Sharifi, F., Arab Amiri, A. R., & Kamkar Rouhani, A. (2019). Using a combination of genetic algorithm and particle swarm optimization algorithm for GEMTIP modeling of spectral-induced polarization data. *Journal of Mining and Environment*, *10*(2), 493-505.

[34]. Thió-Henestrosa, S., & Martín-Fernández, J. A. (2006). Detailed guide to CoDaPack: a freeware compositional software. *Geological Society, London, Special Publications*, *264*(1), 101-118.

[35]. Compositional Data Package, (2022). *University of Girona*

[36]. Stacklies, W., Redestig, H., Scholz, M., Walther, D., & Selbig, J. (2016). pcaMethods—a bioconductor package providing PCA methods for incomplete data. *Bioinformatics*, *23*(9), 1164-1167.

[37]. Dürr, O., Sick, B., & Murina, E. (2020). *Probabilistic deep learning: With python, keras and tensorflow probability*. Manning Publications.

وارون‌سازی داده‌های قطبش القایی طیفی با استفاده از تکنیک‌های شبکه عصبی

پرنیان جوادی‌شریف[۱]، علیرضا عرب‌امیری[۱*]، بهزاد تخم‌چی[۱] و فریدون شریفی[۲]

۱- دانشکده مهندسی معدن، نفت و ژئوفیزیک، دانشگاه صنعتی شاهرود، ایران

۲- دانشگاه کلن، آلمان

ارسال ۲۰۲۴/۰۵/۱۶، پذیرش ۲۰۲۴/۰۸/۳۱

* نویسنده مسئول مکاتبات: alirezaarabamiri@yahoo.com

چکیده:

روش قطبش القایی طیفی با در نظر گرفتن ویژگی‌های فیزیکی ادخال‌های قطبش‌پذیر توانایی شناسایی و تفکیک منابع مختلف ایجاد قطبش القایی را دارد. با این حال شناسایی و تفکیک این ویژگی‌ها با در نظر گرفتن مدل واهلش مناسب امکان‌پذیر است و مدل تئوری محیط موثر تعمیم یافته قطبش القایی (GEMTIP) امکان استخراج ویژگی‌های مختلف و شناسایی منابع مختلف ایجاد قطبش القایی را امکان‌پذیر می‌نماید. با این وجود، زمان محاسبات وارون‌سازی، غیر خطی بودن معادلات و پیچیدگی روابط ازجمله مشکلات وارون‌سازی می‌باشد و برای حل این مشکلات، رویکرد جدید مبتنی بر یادگیری عمیق از طریق شبکه عصبی همامیخت برای محاسبه پارامترهای ادخال‌های قطبش‌پذیر داده‌های قطبش القایی طیفی با استفاده از مدل محیط موثر تعمیم یافته ارئه شده است. شبکه عصبی پیشنهادی با استفاده از ۲۰۰۰۰ مجموعه پارامتر و پاسخ مدل پیشرو آموزش دیده است. درحالیکه شبکه‌های عصبی عمیق، پیچیدگی‌های غیر خطی را نیز در نظر می‌گیرند، با استفاده از تبدیلات لگاریتمی و استخراج مولفه‌های اصلی خطی و غیر خطی نیز سعی در افزایش دقت این وارون‌سازی شده‌است. در مرحله ارزیابی از داده‌های مربوط به منطقه کرویان در جنوب غربی شهرستان سقز استفاده شده‌است. در این منطقه کانی‌های کوارتز و پیریت در کنار یکدیگر دیده‌می‌شود و پیریت‌های منطقه شامل دو نوع درشت‌دانه بدون طلا و ریزدانه طلادار می‌باشد. وجود این کانی‌سازی پیریت با خصوصیات متفاوت فیزیکی، یک هدف جذاب برای بررسی تکنیک پیشنهادی می‌باشد. شبکه آموزش‌دیده‌شده، با استفاده از داده‌های قطبش القایی طیفی منطقه کرویان اعتبارسنجی‌شده و در تفکیک دو عامل ایجادکننده پدیده قطبش القایی‌طیفی با ابعاد ذرات متفاوت موفق بوده‌است. روش پیشنهادی فرآیند وارون‌سازی را در زمان کمتر و با دقت و جزئیات بیشتر انجام‌داده‌است.

کلمات کلیدی: قطبش القایی طیفی، شبکه عصبی همامیخت، تئوری محیط موثر تعمیم یافته، تبدیل لگاریتم مرکزی، تبدیل لگاریتم.